Cell Stem Cell, Volume *27*

Supplemental Information

Androgen Signaling Regulates SARS-CoV-2 Receptor Levels and Is Associated with Severe COVID-19 Symptoms in Men

Ryan M. Samuel, Homa Majd, Mikayla N. Richter, Zaniar Ghazizadeh, Seyedeh Maryam Zekavat, Albertas Navickas, Jonathan T. Ramirez, Hosseinali Asgharian, Camille R. Simoneau, Luke R. Bonser, Kyung Duk Koh, Miguel Garcia-Knight, Michel Tassetto, Sara Sunshine, Sina Farahvashi, Ali Kalantari, Wei Liu, Raul Andino, Hongyu Zhao, Pradeep Natarajan, David J. Erle, Melanie Ott, Hani Goodarzi, and Faranak Fattahi

Figure S1, Related to Figure 1

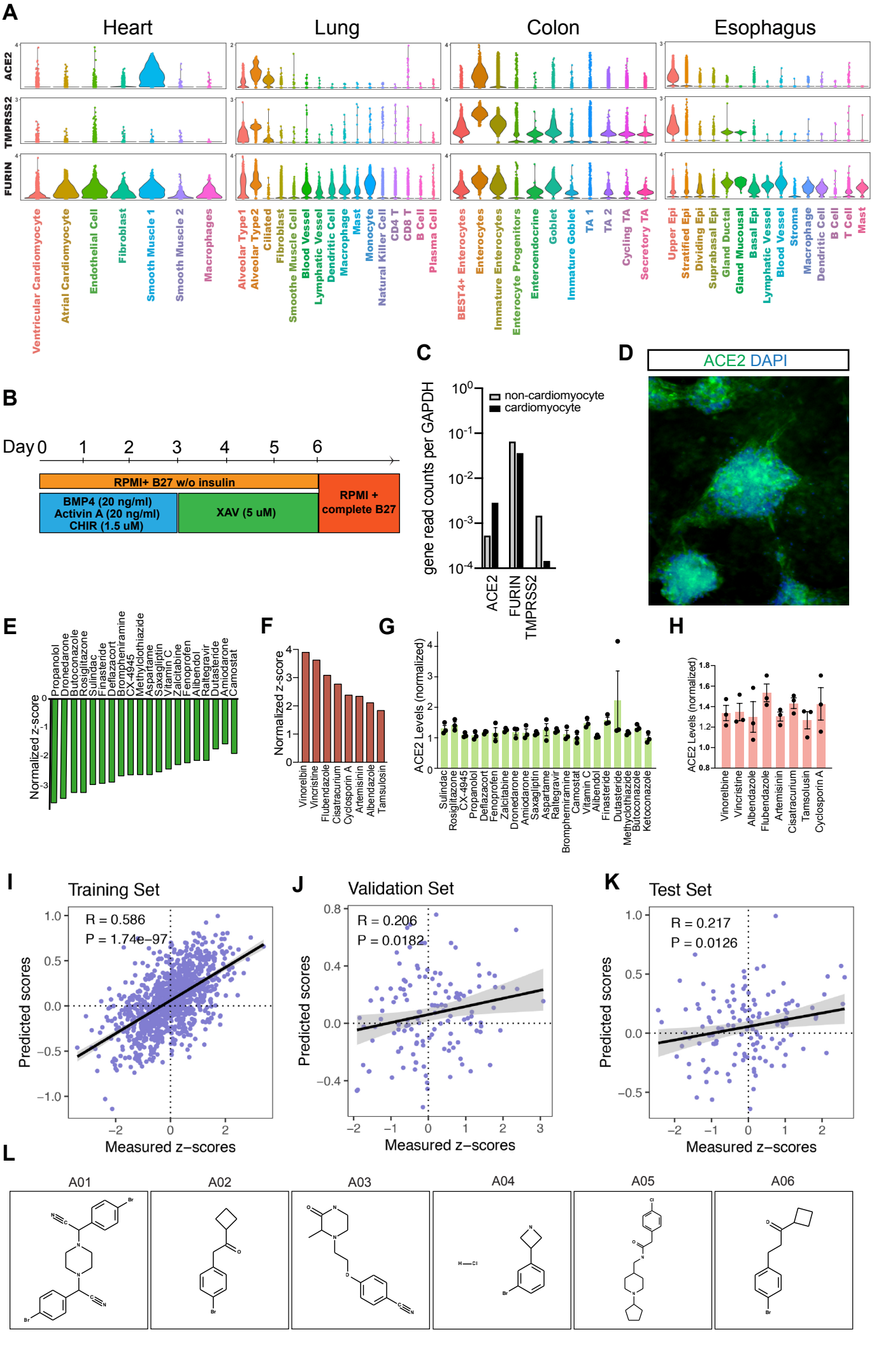

Figure S1. Cell type specific expression of SARS-CoV-2 receptor and its modulation with *in vitro* and *in silico* hit compounds.
Related to Figure 1

(A) Violin plots showing the cell type specific expression of ACE2, TMPRSS2 and FURIN for human adult heart, lung, colon and esophagus. The expression is displayed as the log normalized values.
(B) Schematic representation of cardiac differentiation protocol.
(C) Expression of ACE2, FURIN, and TMPRSS2 in hESC-derived cardiomyocytes and non-cardiomyocytes. Expression is normalized by GAPDH read count.
(D) Immunofluorescence imaging of cardiac cells stained with ACE2 antibody.
(E-F) Normalized z-score of compounds in FDA-approved library that up/down-regulate ACE2 in human cardiac cells.
(G-H) Effect of hit compounds on ACE2 expression levels in Vero cells.
(I-L) Comparison of predicted and measured *z*-scores for the training (I), validation (J) and test (K) datasets in virtual high-throughput screening experiment. Also shown are the Pearson correlation coefficients and their associated *p*-values. (L) Chemical structure of selected *in silico* hit compounds.

Figure S2, Related to Figure 2

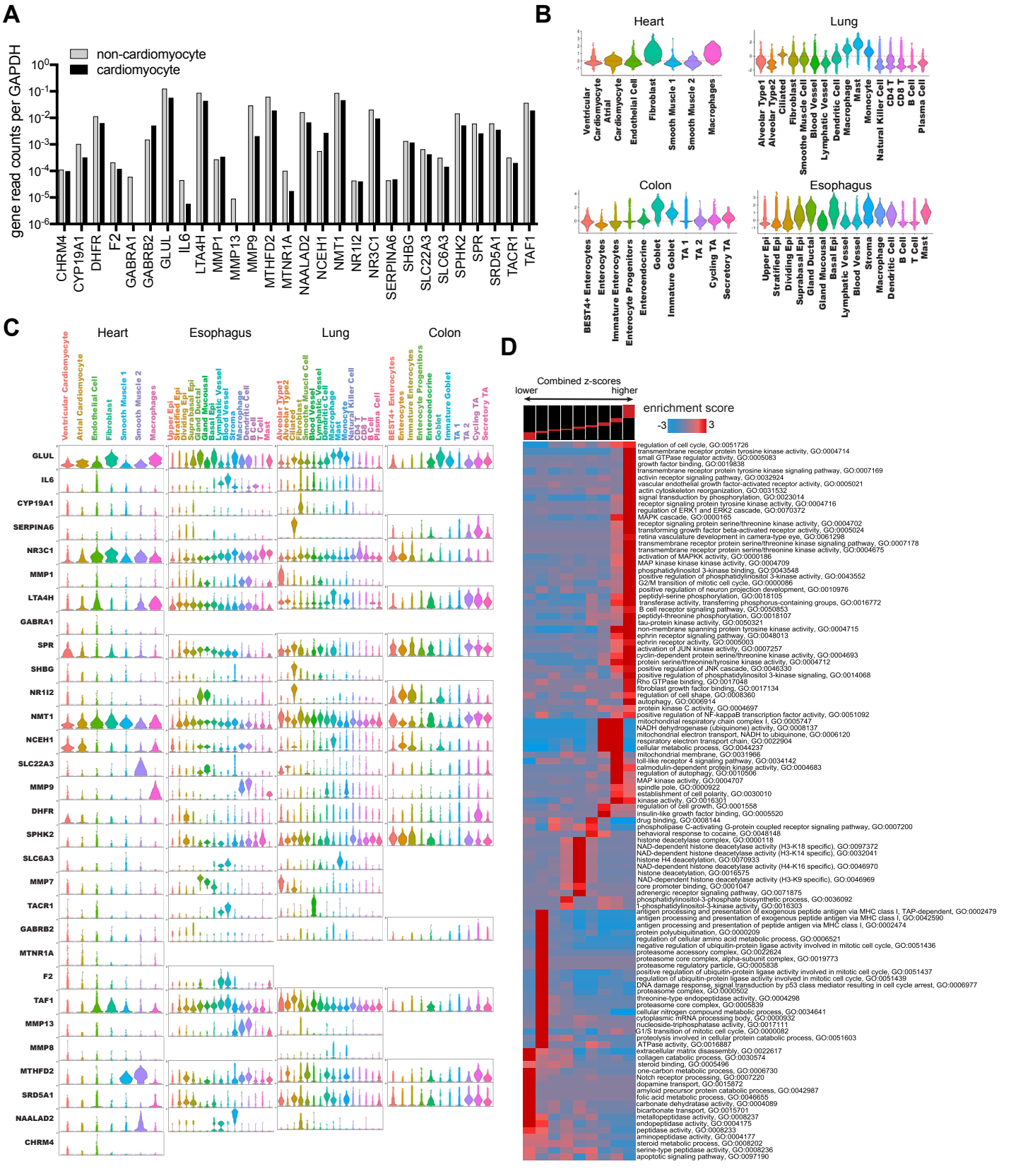

Figure S2. Cell type specific expression of predicted targets and their associated pathways.
Related to Figure 2

(A) Expression of predicted targets in hESC-derived cardiomyocytes and non-cardiomyocytes. Expression is normalized by GAPDH read count.
(B) Violin plots showing the cell type specific module scores for the 30 predicted gene targets for human adult heart, lung, colon and esophagus.
(C) Violin plots showing the cell type specific expression of the 30 predicted gene targets for each organ. The expression is displayed as the log normalized values.
(D) Pathways discovered by iPAGE and their pattern of representation across proteins associated with high/low z-scores in the FDA-approved library screen. Each expression bin includes genes within a specific range of expression values (top panel). Bins to the left contain genes associated with lower z-scores and bins to the right contain genes associated with higher z-scores. Rows correspond to pathways and columns to expression bins. Red entries indicate enrichment of pathway genes in the corresponding expression bin.

Figure S3, Related to Figure 3

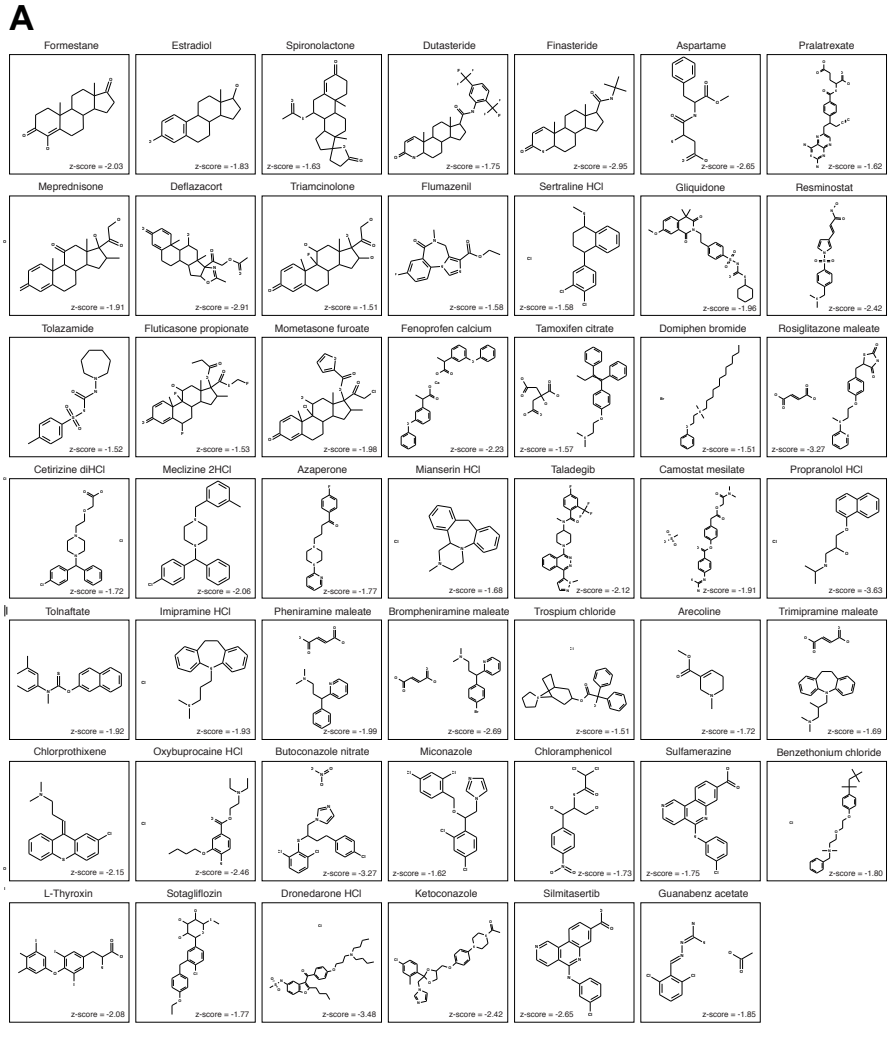

Figure S3. Interaction of hit compounds with target proteins.
Related to Figure 3

(A) Chemical structure of hit compounds that interact with predicted targets. Canonical SMILES and PubChem Sketcher were used to draw the structures.
(B-C) Drug-target interactions in selected GO terms. (B) Drug-protein interaction matrix for GO:0008202 steroid metabolic process gene set. (C) Drug-protein interaction matrix for GO:0008236 serine-type peptidase activity gene set.
(D-G) Cell type specific expression of AR signaling modulators. Violin plots showing the cell type specific expression of AR, SRD5A1, SRD5A2 and cell type specific module scores for 8 RTK's upstream of AR activity, 30 genes associated with the androgen receptor signaling pathway and 34 common downstream targets of AR transcriptional regulatory activity in the human adult heart (D), lung (E), colon (F) and esophagus (G).

Figure S4, Related to Figure 4

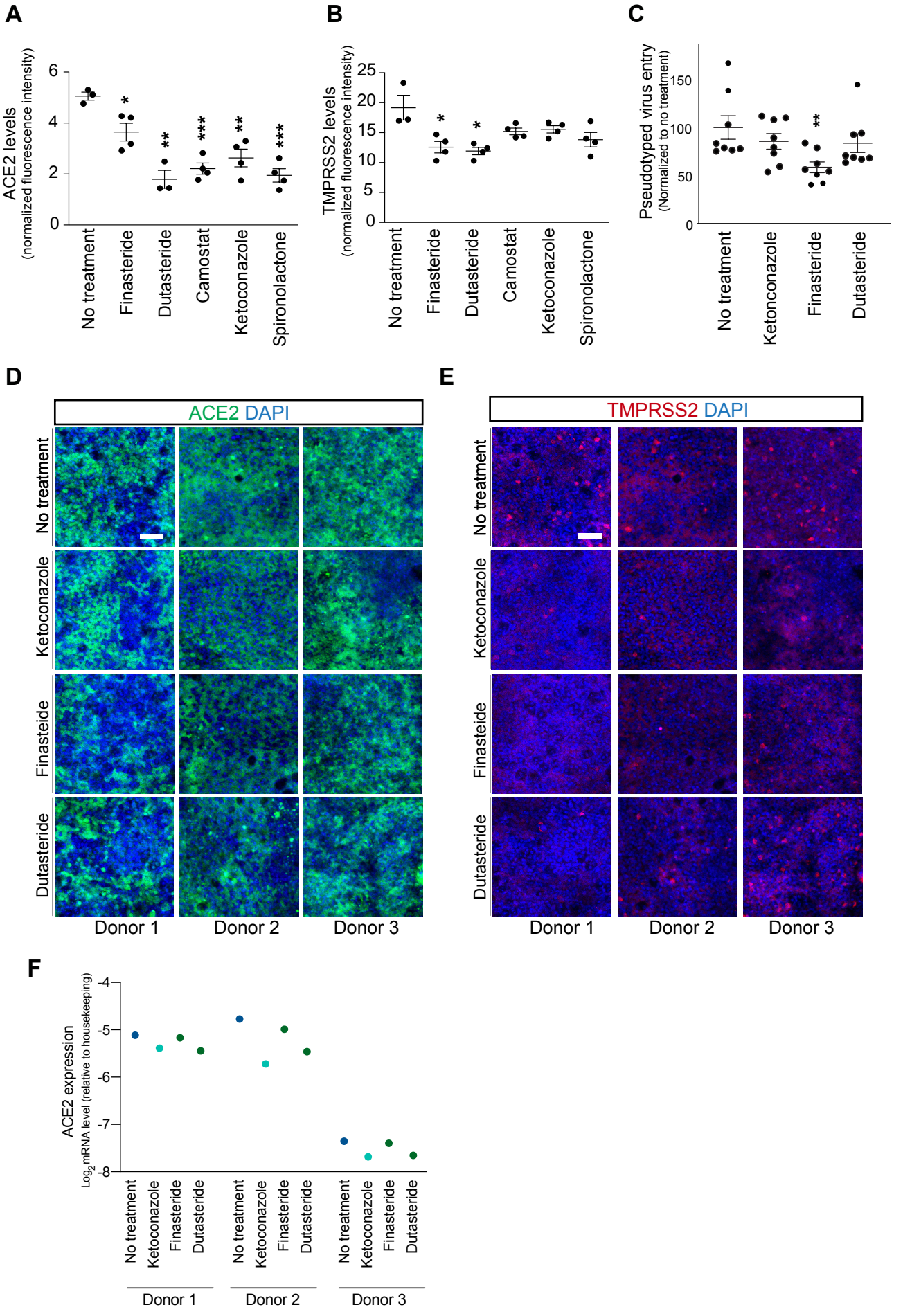

Figure S4. Antiandrogenic drugs reduce SARS-CoV-2 levels and pseudotyped virus entry in target cells. **Related to Figure 4**

(A-C) Effect of AR signaling inhibitors on the expression of ACE2 (A) and TMPRSS2 (B) in hESC-derived cardiac cells. (C) Effect of antiandrogenic drugs on SARS-CoV-2 pseudotyped virus internalization in human primary alveolar epithelial cells.
(D-F) Antiandrogenic drugs reduce ACE2 and TMPRSS2 in human bronchial epithelial cells. (D) Immunofluorescence analysis of ACE2 expression in response to treatment with antiandrogenic drug candidates in primary bronchial epithelial cells isolated from three different donors. Individual values represent normalized fluorescence intensity in independent imaging fields. (E) Immunofluorescence analysis of TMPRSS2 expression in response to treatment with antiandrogenic drug candidates in primary bronchial epithelial cells isolated from three different donors. (F) qRT-PCR analysis of ACE2 mRNA expression in response to treatment with antiandrogenic drug candidates in primary bronchial epithelial cells isolated from three different donors. Scale bar = 100 μm.

Figure S5, Related to Figure 5

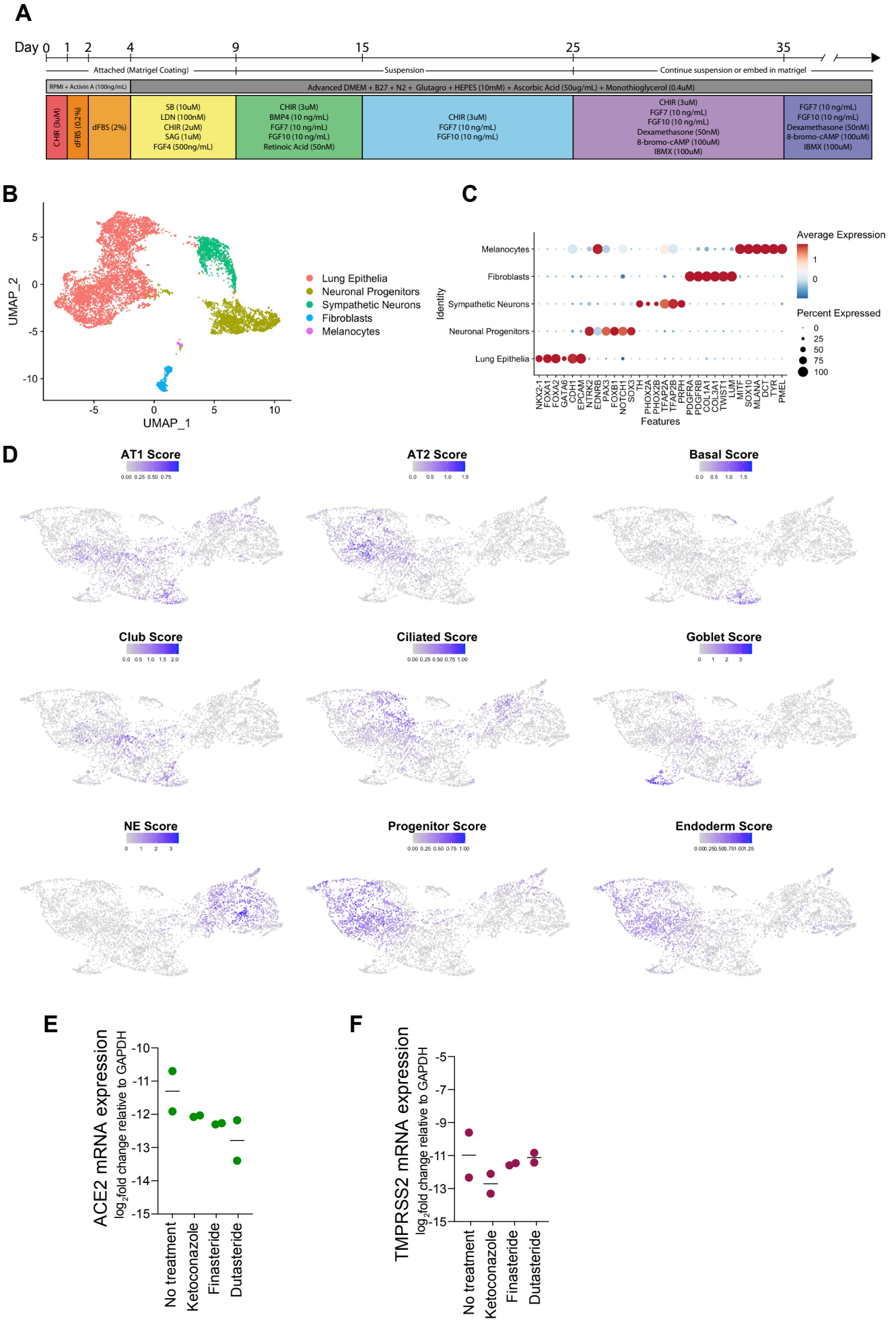

Figure S5. Differentiation and characterization of HLOs for assessment of antiandrogenic drugs.
Related to Figure 5

(A-D) Differentiation and characterization of HLOs. (A) Schematic illustration of HLO differentiation protocol.
(B) UMAP visualization of scRNA-seq data from differentiated HLOs showing distinct cell clusters.
(C) Dot plot visualization of single cell expression of cluster specific lineage markers in differentiated HLOs.
(D) UMAP visualization of module score analysis of different lung epithelial subtypes using panels of lineage specific markers listed in Figure 5B.
(E-F) Effect of antiandrogenic drug candidates on ACE2 and TMPRSS2 expression in HLOs. (E) qRT-PCR analysis of ACE2 expression in HLOs treated with antiandrogenic drugs. (F) qRT-PCR analysis of TMPRSS2 expression in HLOs treated with antiandrogenic drugs.

Figure S6, Related to Figure 6

A

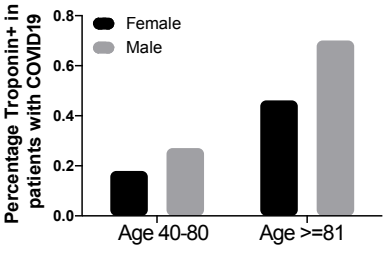

B

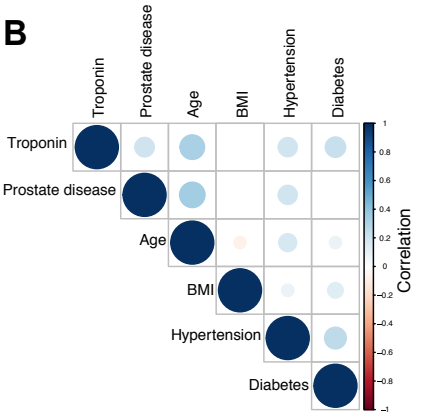

C

	UK Biobank Men
n	190,150
*age (mean (SD))**	56.81 (8.17)
Smoking Status (%)	
Current	23401 (12.4)
Never	92304 (48.9)
Previous	73214 (38.8)
BMI (mean (SD))	27.81 (4.22)
Benign Prostatic Hypertrophy (%)	22834 (12.0)
Type 2 Diabetes Mellitus (%)	19794 (10.4)
Coronary Artery Disease (%)	31902 (16.8)
Hypertension (%)	83510 (43.9)
Chronic Obstructive Pulmonary Disease (%)	11945 (6.3)
Asthma (%)	25513 (13.4)
COVID+ (%)	831 (0.4)
COVID+ and Hospitalized (%)	534 (0.3)

D

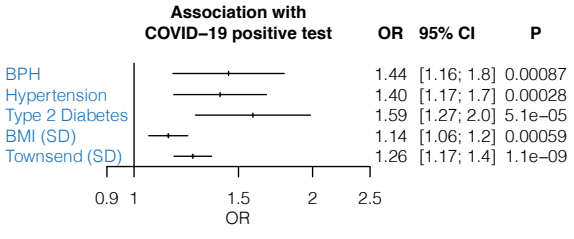

E

	*All Men (COVID Controls)**	*COVID-19 Positive Men*	*COVID-19 Positive & Hospitalized Men*	*p*
N	189319	831	534	
*age (mean (SD))***	56.80 (8.17)	57.25 (8.85)	58.55 (8.47)	<0.001
Smoking Status (%)				<0.001
Current	23299 (12.4)	102 (12.4)	66 (12.5)	
Previous	72839 (38.7)	375 (45.7)	198 (37.6)	
Never	91960 (48.9)	344 (41.9)	262 (49.8)	
BMI (mean (SD))	27.80 (4.22)	28.94 (4.67)	29.20 (4.70)	<0.001
Benign Prostatic Hypertrophy (%)	**22685 (12.0)**	**149 (17.9)**	**113 (21.2)**	
Type 2 Diabetes Mellitus (%)	19611 (10.4)	183 (22.0)	142 (26.6)	<0.001
Coronary Artery Disease (%)	31698 (16.7)	204 (24.5)	154 (28.8)	<0.001
Hypertension (%)	83029 (43.9)	481 (57.9)	336 (62.9)	<0.001
Chronic obstructive pulmonary disease (%)	11848 (6.3)	97 (11.7)	74 (13.9)	<0.001
Asthma (%)	25397 (13.4)	116 (14.0)	76 (14.2)	0.683

F

Gene*	CHR	Pos_Start	Pos_End
CYP19A1	15	51500253	51630795
NR3C1	5	142657495	142783254
IL6	7	22766765	22771621
NCEH1	3	172348434	172429008
SERPINA6	14	94770584	94789688
SHBG	17	7531286	7536701
SRD5A1	5	6633499	6669675
AR	X	66763874	66950461
SRD5A2	2	31749656	31806040

*note: AR not used because X-chromosome was not included in the GWAS analyses

G

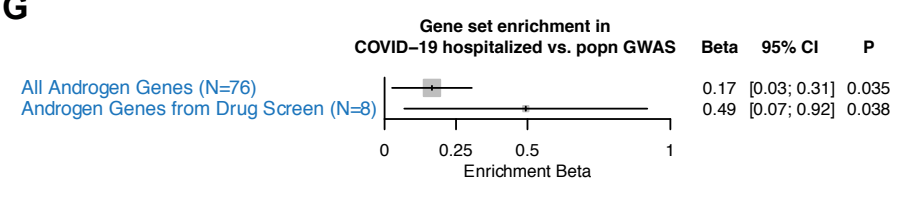

H

SNP	*Effect Allele*	*UKBB Effect Frequency*	*UKBB Genotype INFO score*	*Bioav. Testosterone Effect (SD)*	*Bioav. Testosterone SE*	*Bioav. Testosterone P*	*COVID Cohorts (N)*	*COVID Effect*	*COVID SE*	*COVID P*	*Heterogeneity P-val between cohorts*	*COVID Samples (N)*	*COVID Effect Frequency*
rs17703883	C	0.25	0.995	0.024	0.002	3.60E-27	8	-0.047	0.037	0.22	0.90	900653	0.251
rs28929474	C	0.98	1	0.092	0.007	9.50E-39	4	0.34	0.17	0.047	0.34	864917	0.983
rs17580	T	0.95	1	0.027	0.005	9.90E-09	6	-0.19	0.086	0.027	0.23	870440	0.963
rs545206972	T	0.007	0.973	0.43	0.012	1.80E-265	3	0.48	0.29	0.094	0.84	863380	0.007
rs1799941	G	0.74	0.993	0.063	0.002	5.20E-169	8	0.04	0.038	0.29	0.16	900653	0.743
rs113017476	A	0.039	0.981	0.087	0.005	7.80E-65	5	-0.062	0.11	0.56	1.00	652738	0.038

I

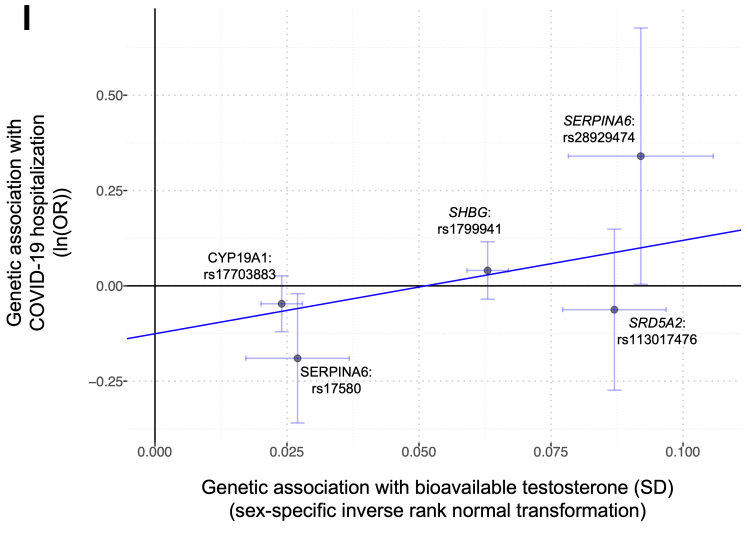

Figure S6. The role of androgen signaling in COVID-19 susceptibility and severity in male patients. **Related to Figure 6**

(A-B) Effects of risk factors on abnormal troponin T in COVID-19 patients. (A) Distribution of sex among patients with abnormal troponin T. (B) Correlogram of variables in the Yale COVID-19 patients dataset. The size and color of each circle illustrates the direction and strength of the correlation. Only significant correlations (at $p<0.05$) are painted.

(C-E) Patient record analysis of COVID-19 susceptibility and severity in the UK Biobank. (C) UK Biobank summary statistics across men used in analysis. Age refers to age at enrollment in 2010. (D) Association of BPH with COVID-19 susceptibility in multivariate logistic models adjusted for age, hypertension, type 2 diabetes, normalized body mass index (BMI), Townsend deprivation index, and principal components of genetic ancestry. (E) UK Biobank summary statistics across men used in analysis, stratified by COVID+ status as of 9/22/2020. * Controls included all white British men from the UK Biobank English recruitment centers who either tested negative for COVID-19 or did not have a COVID-19 test. ** Age refers to age at enrollment in 2010. OR = odds ratio, CI = confidence interval.

(F-G) Mendelian randomization analysis of androgen signaling related genes in UK Biobank. (F) List of androgen signaling target genes identified in drug screen. (G) Sensitivity analysis for MR-Egger Mendelian randomization analysis of bioavailable testosterone with COVID-19 hospitalization. Mendelian randomization analysis between bioavailable testosterone and COVID-19 hospitalization variants near the androgen genes excluding the top SHBG variant from Figure 6E.